Energy Exchange During Electron Emission from Carbon Nanotubes: Considerations on Tip Cooling Effect and Destruction of the Emitter

M. Dionne*, S. Coulombe and J.-L. Meunier
[1]Department of Chemical Engineering, McGill University
*Corresponding author: 3610 university street, Montréal, Québec, Canada, H3A 2B2

Abstract: Murphy and Good general theory for electron emission from metal surfaces was used to predict the field-emission capabilities of ideal arrays of vertically aligned carbon nanotubes (VACNT). The Nottingham effect was taken into account in order to explain experimental observation of a localized cooling of the VACNT tips during field emission and the total destruction of very short emitters at strong currents. Our model allowed to match the current, voltage and observed breaking points of individual VACNT reported in two separate experimental studies.

Keywords: Carbon nanotubes, field emission.

1. Introduction

Electron emission from metal surfaces is driven by high temperatures T_s or strong electric fields E_s. It is usually categorized into three regimes known respectively as field emission (negligible temperatures, strong fields), thermionic emission (high temperatures, weak to negligible fields) and thermo-field (T-F) emission (high temperatures, strong fields). A general theoretical description of electron emission was provided by Murphy and Good (M-G) [1] and later verified experimentally [2]. M-G theory provides a complex integral expression for the electron current density J_{M-G} that can only be evaluated numerically. As a consequence, the much simpler Fowler-Nordheim [3] and Richardson-Dushman [4] analytical equations are widely used respectively for field (J_{F-N}) and themionic (J_{R-D}) emission. Since these equations originate from simplifications of the M-G theory, they can be expected to digress from the actual J_{M-G} prediction, especially as the T-F regime is approached. Our previous work [5] demonstrated that J_{R-D} always underestimates J_{M-G} significantly and thus, we concluded that the use of the M-G equation is necessary for $E_s = 10^{7-10}$ V/m, T_s=1000-5000 K and for all values of the work function ϕ_0.

The local field enhancement factor, $\beta \equiv |E| / E_0$, indicates how strongly electron emission is enhanced by long, sharp structures such as vertically aligned carbon nanotubes (VACNT). These materials seem ideal for new electrodes optimized for field emission because they produce high β values on their tips and are excellent conductors [6]. The ability to emit strong electron currents at low surface temperatures may allow the creation of a new family of low erosion electrodes for high current applications. In a more recent paper [7] we compared J_{F-N} to J_{M-G} based on a discussion from [8] where it was pointed out that F-N equation underestimated J_{M-G} by a factor $10^{2\text{-}6}$ at 1000 K and above. Our calculations indicate that for the particular value ϕ_0=4.5 eV used for carbon nanotubes (CNT), a nearly constant factor of 10^2 was found. It appeared then necessary to use J_{M-G} in all circumstances. In [9] the current-induced destruction of CNT field emitters was studied in an attempt to include the heat exchange associated to electron emission. In this study, Richardson theory was used to suggest that each electron was removing an energy $\varepsilon = 1.5 k_B T_s$ where T_s is the surface temperature. The consequence of this assumption was a localized cooling of the CNT tip during field emission partially compensating for the Joule heating. The longitudinal temperature profile then showed a peak with a maximum value occurring somewhere along the CNT body. Once this peak temperature reached a critical value that could initiate the etching of carbon by trace amounts of oxygen, a breaking of the CNT was predicted at this location. Therefore, it was deduced that a section of the emitter would be taken away. When this effect was not included,

the hottest point was located at the CNT tip and the predicted tip-based destruction mechanism was referred to as field-assisted evaporation [10]. Although we agree with the idea that high temperatures are responsible for the destruction of CNT during field emission, we do not believe it is advisable to use results from Richardson's theory while still assuming strong surface fields to be present. M-G theory also provides a more valid description of the energy loss or gain experienced by the crystalline lattice of a given material during the emission process. This phenomenon, known as the Nottingham effect (see [8]) can either heat or cool the surface depending on whether the replacing electron coming from the external circuit has a greater or lower energy than the emitted electron.

In this paper we first discuss the achievable surface-averaged current density I_{eq} (A/m^2) predicted by M-G theory for VACNT arrays of different length h and radius r, assuming a constant spacing Δx between ideal emitters in good electrical and thermal contact with a copper substrate. The combined contributions of Joule heating and the Nottingham effect on the longitudinal temperature profile within the emitters are then discussed. The complex dependency between the role of the Nottingham effect (either a cooling or a heating effect) and the local values of E_s and T_s during an applied field (E_0) ramp is then used to explain the apparent validity of the $\varepsilon = 1.5 k_B T_s$ assumption for the emitted electrons in some circumstances. However, the greater range of validity of M-G theory allowed us to suggest a simple explanation for the final stages of the emitters destruction described in [9], which proved inconsistent with the authors' predictions. A significant part of our attention was focussed on these apparently problematic cases characterized by smaller aspect ratios ($h/r \leq 20$).

2. Theory

In this section we discuss the M-G theory and the predicted values of J_{M-G}. The Nottingham energy exchange term ε_{Not} (in eV) representing the energy gain (or loss) experienced by the surface is also discussed. These results are first studied independently before including them in our set of governing equations.

For a complete description of the electron emission process, we refer the reader to the original work of Murphy and Good [1] as well as [8] and of our preceding work [5, 7]. J_{M-G} is given by Equation 1.

$$J_{M-G} = e \int_{-W_a}^{\infty} D(E_s, W) N(W, T_s, \phi_0) dW \qquad (1)$$

$-W_a$ is the effective constant potential inside the emitter, W is the energy of an incident electron on the potential barrier in the perpendicular direction to the surface, $D(E_s,W)$ is the probability for the electron of energy W to penetrate the barrier and $N(W,T_s,\phi_0)$, is the number of Fermi-Dirac electrons within the dW energy interval. Once J_{M-G} is known, Fermi-Dirac statistics can be used to provide ε_{Not} as indicated by equations 2-4 where $E = p^2/2m_e + V$ is the total energy of an electron.

$$\varepsilon_{Not} = \frac{e}{J_{M-G}} \int_{-\infty}^{\infty} E P_E(E, E_s, T_s, \phi_0) dE + \phi_0 \qquad (2)$$

$$P_E(E, E_s, T_s, \phi_0) = \int_{-\infty}^{E} N_E(E, T_s, \phi_0) D(E_s, W) dW \qquad (3)$$

$$N_E(E, T_s, \phi_0) = -\frac{4\pi m_e}{h^3} \frac{1}{1 + \exp\left(\frac{E + \phi_0}{k_B T_s}\right)} \qquad (4)$$

In equation 2 the second term (ϕ_0) is equal to the energy of the replacing electron (i.e. the Fermi energy ε_F). p and V are respectively the momentum and potential energy of the electron. P_E is the probability for the number of electrons N_E having an energy E to penetrate the potential barrier. A simple interpretation of this balance equation is that if the applied field is strong enough, more electrons are emitted even though they originate from energy states located below the Fermi energy. The energy difference between the newly available states and ε_F is then transmitted to the lattice when the replacing electrons occupy these available low energy states first. On the other hand, at high surface temperatures the number of electrons having an energy larger than ε_F is significant enough to supply most of the emission current and the replacing electrons must absorb energy from the

lattice in order to occupy the only states available. Electron emission thus becomes a cooling mechanism under these circumstances.

3. Governing equations

In this section we discuss the differential equations defining our problem. The boundary conditions and the key assumptions are also introduced.

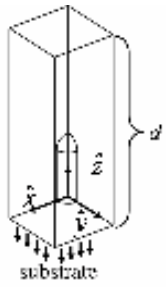

Figure 1: A single VACNT on the substrate.

Figure 1 shows a VACNT standing at the origin of a 3-D Cartesian grid on the metal substrate. When a potential difference ΔV is applied between this surface and a flat anode located at a distance d, the magnitude of the electric field $\left|\vec{E}\right|$ close to the cathode surface is greater than the value of the 1-D solution ($E_0 = \Delta V/d$) one finds between two infinite flat electrodes. To quantify this effect, the field enhancement factor $\beta = \left|\vec{E}\right|/E_0$ is defined. For a VACNT-shaped structure as shown in fig. 1, the Laplace equation can be solved above the cathode surface to provide the 3-D β profile. To simulate the presence of other elements of the VACNT array, symmetry conditions can be assumed at the limits of the computational domain along the $\hat{x}$ and $\hat{y}$ axes. It has been reported previously [11] that $\beta = 1.2\left(2.15 + (h/r)_{CNT}\right)^{0.9}$ on the tip of isolated VACNT, where $(h/r)_{CNT}$ is the ratio between the length (or height, h) and radius (r) of the structure of interest (i.e. the aspect ratio). It is also known [12] that when two identical VACNT stand close to each other within a distance Δx similar to h, the value of β on the surface decreases. This phenomenon results from screening effects and causes the value of I_{eq} for the array to decrease when the VACNT are brought closer. On the other hand, when $\Delta x >> h$, the lower number of emitters contributing to I_{eq} also reduces this value. As a consequence, an optimal spacing $\Delta x_{optimal}$=(1 to 2)h is found. We used this information in the study of three different theoretical arrays as well as experimental data for isolated VACNT [9, 16].

Table 1: Description of the CNT dimensions

Designation	h_{CNT} (nm)	r_{CNT} (nm)	$(h/r)_{CNT}$
$(h/r)_{CNT}$=100	5000	50	100
$(h/r)_{CNT}$=20	1000	50	20
$(h/r)_{CNT}$=5	100	20	5
1	470	7	67.1
2	330	7	47.1
Doy_1	1000	10.5	95.2
Doy_5	100	2.6	38.4

In order to calculate the emitter temperature, the current and heat conservation equations were solved within the cathode volume using accepted CNT electrical and thermal properties (see [13]) and experimental data from [9, 16]. Symmetry conditions were also used at the limits along the $\hat{x}$ and $\hat{y}$ axes. We assumed V=0 at the lower boundary along $\hat{z}$ and the value of $\left|\vec{E}\right|$ on the cathode surface was used to dictate a current density boundary condition with equation 1. To that end, we used COMSOL "Electrostatics" model to calculate $\left|\vec{E}\right|$ in the inter-electrode volume and the "Conductive media DC" model inside the electrode. A heat flux condition defined as $\left|\vec{q}\right| = J_{M-G} \cdot \varepsilon_{Not}$ was also defined to include the Nottingham effect. The Stefan-Boltzmann equation was used to calculate radiation losses. The temperature at the lower boundary along $\hat{z}$ was set to 300 K. Unlike in the case of hot thermionic emitters subjected to relatively low ($10^{7\text{-}8}$ V/m) surface fields, the contribution of the Nottingham effect could not be predicted intuitively. For hot emitters, one can expect at first a heating effect to occur until the increasing number of electrons emitted from energy states higher than ε_F allows the Nottingham effect to become a cooling effect. This turning point, referred to as the inversion temperature T_{inv}, could lead us to expect the same scenario to take place in cold emitters. However, when no external heat source is used

to impose a high temperature, the actual value of T_s (either above or below T_{inv}) depends on the intensity of the local Joule heating which in turn depends on the effective value of E_s. In the case of very weak emitted currents, the negligible contribution of Joule heating (proportional to $\left|\vec{J}\right|^2$) may indicate the Nottingham effect-induced heat flux, proportional to $\left|\vec{J}\right|$, would also be dissipated by heat conduction.

4. Results and discussion

In this section we first study the $J_{M\text{-}G}$ and ε_{Not} data independently to formulate a qualitative prediction of the contribution of the Nottingham effect during field emission and when both E_s and T_s are high. We then show the $I_{eq}(E_0)$ curves for our theoretical arrays of interest in order to evaluate their ideal theoretical performances. The corresponding ε_{Not} data is then extracted to understand the evolution of the Nottingham effect between its two possible regimes (cooling or heating). The transition between these two regimes is then used to explain how an overheating VACNT array would be destroyed progressively. Finally, case studies are performed for individual VACNT described in [9] to demonstrate how our model can be used successfully to predict the observed locations of the CNT breaking points x_B (nm) measured from the CNT base.

Figures 2 and 3 show respectively the values of $J_{M\text{-}G}$ and ε_{Not} as functions of E_s and T_s obtained from equations 1 and 2. In [8], these results were provided above 1000 K and as fig. 2 indicates, large current densities may result from pure field emission at low temperatures once $E_s>10^9$ V/m. In the resolution process, the system of equations became unstable if negligible current densities were extracted from calculated $J_{M\text{-}G}(E_s,T_s)$ data tables. The simplest counter-measure to this problem was to add an arbitrary 10^{-10} A/m^2 contribution and to disregard I_{eq} data of the same magnitude. In fig. 3, we see that this assumption had an effect on the value of ε_{Not} by preventing the possible division by $J_{M-G} \approx 0$ in front of the integral in equation 2. The $\varepsilon_{Not}>0$ area depicted in fig. 3 indicates that the Nottingham effect acts as a cooling mechanism whereas for $\varepsilon_{Not}<0$, it is heating the surface. Based on this information, a plausible scenario can be suggested. First, a small heating effect may take place. Then, as T_s increases for intermediate E_s values, a cooling effect could occur on the VACNT tips but ultimately this effect would be lost as $E_s \to 10^{10}$ V/m because the value of T_{inv} becomes very large. The results of fig. 3 show that the addition of 10^{-10} A/m^2 to $J_{M\text{-}G}$ caused ε_{Not} to approach the work function value at low temperatures $\varepsilon_{Not} \to \phi_0 = 4.5eV$. This occurred only for $J_{M-G} \approx 10^{-10}$ A/m^2. Keeping in mind that the real calculated value of $J_{M\text{-}G}$ was even smaller, the Nottingham effect could be assumed to be negligible. Indeed, as our initial solutions were computed at low E_0 (with ε_{Not}=4.5 eV) the emitter temperature remained around 300 K.

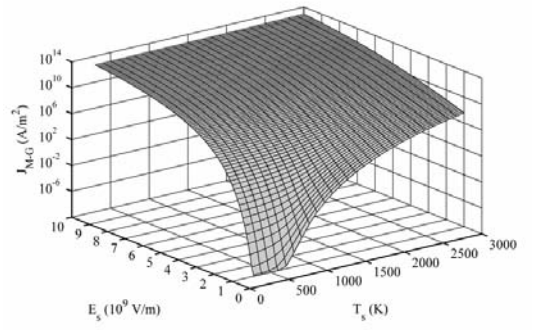

Figure 2: $J_{M\text{-}G}$ as a function of E_s and Ts.

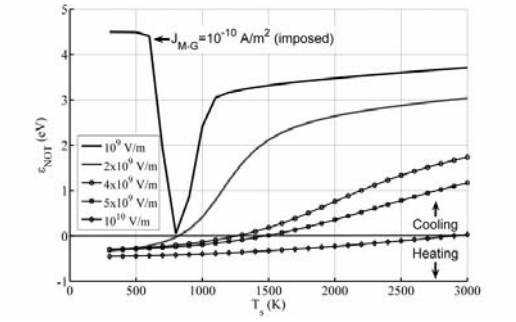

Figure 3: ε_{Not} as a function of T_s for several E_s.

Figure 4 shows the $I_{eq}(E_0)$ curves for the three first arrays indicated in Table I. It can be seen that shorter and denser arrays can reach higher surface-averaged current densities due to an increased number of emitters sharing the total current while still being consistent with the definition of $\Delta x_{optimal}$ in units of h. As a

consequence, we identified the $(h/r)_{CNT}$=5 case as the most promising geometry for achieving very strong currents. The maximum achievable I_{eq} values depend on the assumptions we make on the acceptable temperature limits. We used previous reports [14] on the detrimental effects of air on the CNT structure between 700 and 1000 K to suggest a temperature limit of 600 K . If on the other hand a vacuum environment is assumed, the same effect would require that higher temperatures (1500-2000 K) are needed for these destructive effects from trace amounts of oxygen or water. We also used the results from [15] to estimate the acceptable local current density.

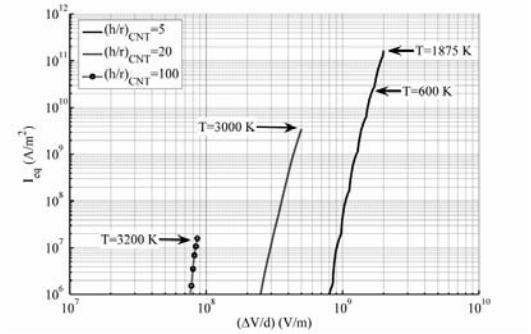

Figure 4: I_{eq} as a function of E_s for three different geometries (ϕ_0=4.5 eV) .

For the particular study described in [9] where the high vacuum environment of a transmission electron microscope was used, temperatures around 2000 K were made accessible. Therefore, we allowed the possibility of reaching 3000 K in our calculations, however for typical experimental conditions, we do believe much lower temperatures should be viewed as acceptable to allow reproducible emission currents. Finally, because the M-G theory is valid for $E_s \le 10^{10}$ V/m, we did not allow this value of E_s to be exceeded when assuming large values for E_0. This forced to the elimination of some data from [16] for which we could estimate $E_s \approx 2\times10^{10}$ V/m. During the E_0 ramp, the value of ε_{Not} travels in the (E_s, T_s) space defined by fig. 3 as dictated by the effective value of T_s. Figure 5 shows the evolution of ε_{Not} for all three theoretical geometries as a function of the normalized applied field. To facilitate the representation, all values of the applied field, which vary from one array to another, were divided by the maximal value of E_0 for each ramp. For $(h/r)_{CNT}$=20 and 100, this value was the one for which T_s=(3000-3200) K but for $(h/r)_{CNT}$=5, T_s only reached 1875 K as the E_s=10^{10} V/m limit was reached first.

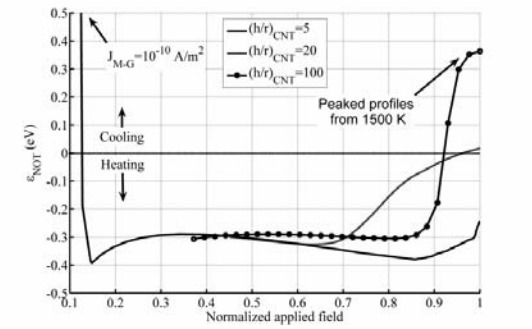

Figure 5: ε_{Not} as a function of the normalized applied field for three different geometries (ϕ_0=4.5 eV) .

One can make a key observation from the ε_{Not} curves: not all arrays experience a significant cooling due to the Nottingham effect. The longest array does go through a phase where ε_{Not}>0 when T_s lies above 1500 K. The magnitude of the Nottingham effect is then sufficient to create a peaked T_s profile along the CNT axis. Keeping in mind that at room temperature (i.e. 300 K) $\varepsilon = 1.5k_BT_s \approx 1/40$ eV one can also estimate that for an increase by a factor 10 in T_s, $\varepsilon = 1.5k_BT_s$ happens to be a good approximation of ε_{Not} in the 1500-3200 K interval. However, the later assumption fails to predict the local heating we now see as the rule rather than the exception below $(h/r)_{CNT}$=20 for ϕ_0=4.5 eV. The $(h/r)_{CNT}$=20 case illustrates very well the limit between the cooling and heating due to the Nottingham effect. In that particular case (h=1 μm) only a small peak in the longitudinal temperature profile can be found near the tip and this only for T_s=3000-3200 K. To understand the differences between the arrays one must study the β profile on the CNT cap surface. As $(h/r)_{CNT}$ decreases, the value of β falls from its maximal value more rapidly across the CNT cap. As a consequence, the fraction of the tip surface effectively acting as an emitting area decreases for lower values of $(h/r)_{CNT}$ and becomes more concentrated at the very tip of the VACNT. These differences impose different heat flux distribution that can only be revealed using a 3-D model where the β values are computed accurately around the emitters. In other words,

only a 3-D model properly representing the $\beta(x,y,z,(h/r)_{CNT},\Delta x)$ structure allows one to observe this effect. One of the consequences is that for two different $(h/r)_{CNT}$ values where r and Δx are the same, matching the βE_0 product on the CNT tips of the two arrays by adjusting E_0 does not produce the same I_{eq}. The shorter array requires a small additional increase in E_0 to compensate for the reduction of the emissive area and so the local values of E_s in its emissive area are higher once the two values of I_{eq} are equal. Fig. 3 indicates that larger E_s are associated with higher T_{inv} values. For $E_s=10^{10}$ V/m the value of T_{inv} is close to 3000 K. Since the $(h/r)_{CNT}=5$ array reaches this surface field below 2000 K it cannot be cooled and for $(h/r)_{CNT}=20$, ε_{Not} only becomes slightly positive at the end of the ramp. As a consequence, the very small peaks are observed in the temperature profile and they are located close to the tip.

We can then conclude that $(h/r)_{CNT}=20$ is a good estimate of the location of the transition point (for $\phi_0=4.5$ eV) between two different destruction mechanisms for the VACNT. Above this point, the presence of peaked longitudinal temperature profile shifts the maximal temperature away from the emitting tip into the CNT body. As a consequence, once the critical temperature is reached for the etching of carbon due to trace amounts of oxygen or water, the emitter will break at this point. Therefore, whole pieces of the CNT will be removed and a new cap will form at the tip of what is left. If the applied field increases again to create a new (still peaked) temperature profile, a shorter CNT piece will be removed. As this process is repeated, the decreasing $(h/r)_{CNT}$ value will at some point approach the $(h/r)_{CNT}=20$ limit. The breaking point will then either be inside the cap or at its boundary with the CNT body (50 nm (=r) from the tip) if we can assume $T_s \approx 3000$ K is accessible. For lower $(h/r)_{CNT}$ values the Nottingham effect only heats the emitters. The $\varepsilon = 1.5 k_B T_s$ assumption only allows a cooling of the surface so stronger fields are regarded as acceptable. Because $\varepsilon_{Not}<0$ the emitters are in fact destroyed from their tip and the total heat source is underestimated.

The last step of our work was to predict the location of the CNT breaking points for the samples described in [9, 16] (see Table 1). In order to adequately represent the experimental conditions, the CNT room temperature resistivity was changed from the value used in [13] (and so far in our work) to the measured value 8.1395×10^{-5} Ωm. We also had to replace the assumption of a good thermal conduction path between the CNT and the substrate by the empirical expression for the heat loss into a tungsten micro-tip (see [9 and 13]). This change reduced by about 50% the current carrying capabilities for case 1 and because more energy was trapped into the CNT, ε_{Not} became positive at lower applied fields due to the higher temperature. Finally, the overall temperature gradient along the CNT was reduced and the temperature at the CNT base increased significantly. From their I-ΔV data, the authors of [9] predicted a maximal temperature T_{max} (about 2000 K) along the CNT located close to the observed breaking point. Under these circumstances, besides predicting the position of this breaking point, it was possible for us to confirm our $\phi_0=4.5$ eV assumption by matching the I-ΔV data within 5-10% for ΔV and within a few μA for I. This error could be justified by the uncertainties on the CNT dimensions, possible current leaks and limited accuracy in the measurements of very small currents. Again, according to [6], $\phi_0=4.5$ eV is an advisable compromise since the possible presence of adsorbed water molecules, trace amounts of metal atoms (see [17 and 18]), graphitic plane edges or other atoms left on or bonded to the CNT during their fabrication and (or) preparation can induce significant variations. We found that only small adjustments were necessary. Reducing ϕ_0 has two consequences. First, it allows the current to be stronger at lower voltages. On the other hand, all inversion temperatures are increased. For example, if we consider $\phi_0=4.0$ eV we find that for the first four curves of fig. 3, T_{inv} is shifted between 800 and 1800 K while for the limiting case $E_s=10^{10}$ V/m, T_{inv} is close to 3500 K. The overall effect however was a greater occurrence of peaked temperature profiles at lower ϕ_0 because $J_{M\text{-}G}$ increased more rapidly with respect to E_s than T_{inv}. As a consequence, the relevant range of $J_{M\text{-}G}$ values was shifted to the region of the (T_s, E_s) space for which $\varepsilon_{Not}>0$. The predicted and observed values of the CNT breaking point z_B

(nm) measured from the CNT base and I along with the predicted values of $T(z_{B(th)})$ and corrected values of ϕ_0 are provided in Table 2. As our data suggest, ϕ_0=4.0 eV was in fact already too low except for case Doy_5. This case was particularly interesting because despite the relatively low ϕ_0 value (3.0 eV) which proved necessary to match the I-ΔV data, ε_{Not} did not become positive until ΔV=244.5 V. At ΔV=246 V the CNT temperature increased almost uniformly above 2000 K over approximately 50% of the CNT length. From 246 to 250 V, the predicted current doubled and more than 90% of the CNT length was heated above 2000 K. This suggests a rapid and total destruction of the emitter at this point because only a small relative change to ΔV triggers it and most of the CNT is affected.

Table 2: Predictions of z_B

Name in [9, 16]	z_B (nm)	$z_{B(th)}$ (nm)	I_{exp} (μA)	I_{th} (μA)	T_{MAX} (K)	ϕ_0
1	390	393	35	39.6	2145	4.3
2	280	282	40	45.6	2015	4.1
Doy_1	900	900	18	35.8	2020	4.8
Doy_5	-	>57	20	27.1	2010	3.0

5. Conclusion

We used M-G theory to predict the electron emission current from ideal VACNT arrays. The Nottingham effect was also taken into account. Its evolution between a heating and a cooling effect during field emission at high (1500-3200 K) temperatures allowed us to propose a new interpretation for the current-induced destruction process of VACNT arrays. This mechanism would be characterized by a significant cooling of the tips for long, thin ($(h/r)_{CNT}$>20) emitters that would be broken at their hottest point. This process would remove CNT sections of decreasing length from one breakup to the other until, below aspect ratios of 20 (ϕ_0=4.5 eV), the breaking point would be once again located in the CNT tip or at the tip itself. This change would be caused by a different contribution of the Nottingham effect which would only heat the emitters throughout the applied field ramp. For lower values of ϕ_0 the tip cooling effect would still be predicted for lower $(h/r)_{CNT}$. However in this case the reduced CNT volume would allow a thermal runaway to occur due to small voltage fluctuations, affecting at least 50% of the CNT length. This particular result and the predicted reversal of the cooling effect provides an explanation of the unexpected total destruction of short emitters reported. For more conventional values of ϕ_0 the Nottingham effect would heat the surface of short emitters instead of cooling it, and the emitter tip would become effectively the hottest point for the weaker applied fields expected.

7. References

[1] Murphy E L and Good R H, 1956, *Phys. Rev.*, **102**, 1464.

[2] Christov S G and Vodenicharov C M, 1968, *Solid-State Electron.*, **11**, 757.

[3] Fowler R H and Nordheim L W, 1928, *Proc. R. Soc. London Ser A*, **119**, 173.

[4] Richardson O W, 1903, *Philos. Trans. R. Soc.*, **201**, 497.

[5] Coulombe S and Meunier J-L, 1997, *J. Phys. D: Appl. Phys.*, **30**, 776-780.

[6] Bonard J-M, Kind H, Stöckli T and Nilsson L-O, 2001, *Solid-State Electron.*, **45**, 893-914.

[7] Dionne M, Coulombe S and Meunier J L, 2008, submitted to *J. Phys. D: Appl. Phys.*

[8] Paulini J, Klein T and Simon G, 1993, *J. Phys. D: Appl. Phys.*, **26**, 1310.

[9] Wei W, Liu Y, Wei Y, Jiang K, Peng L-M, Fan S, 2007, *Nano. Lett*, **7** (1), 64-8.

[10] Dean K A, Burgin T P and Chalamala B R, 2001, *Appl. Phys. Lett.*, **79**(12), 1873-5.

[11] Edgcombe C J and Valdrè U, 2001, *Journal of Microscopy*, **203** (2), 188-94.

[12] Nilsson L, Groening O, Emmenegger C, Kuettel O, Schaller E and Schlapbach L, 2001, *Appl. Phys. Lett.*, **76**(15), 2071-3.

[13] Huang N Y, She J C, Chen J *et al*, 2004, *Phys. Rev. Lett.*, **93** (7), 075501.

[14] Brukh R and Mitra S, 2007, *Journal of Materials Chemistry*, **17**, 619-23.

[15] de Pablo P J, Graugnard E, Walsh B, Andres R P, Datta S and Reifenberger R, 1999, *Appl. Phys. Lett.*, **74** (2), 323-5.

[16] Doytcheva M, Kaiser M and de Jonge N, 2006, *Nanotechnology*, **17**, 3226-33.

[17] Meng T, Wang C-Y and Wang S-Y, 2006, *J. Phys.: Condens. Matter.*, **18**, 10521-8.

[18] Lee Y-H, Kim D H, Kim D H, Ju B-K, 2006, *Appl. Phys. Lett.*, **89**, 083113.